*Article*

# Effect of Ultrasonic Treatment in the Static and Dynamic Mechanical Behavior of AZ91D Mg Alloy

**Helder Puga [1],\*, Vitor Carneiro [2],†, Joaquim Barbosa [1],† and Vanessa Vieira [2],†**

[1]  Centre for Micro-Electro Mechanical Systems (CMEMS), University of Minho, Campus of Azurém, 4800-058 Guimarães, Portugal; E-Mail: kim@dem.uminho.pt

[2]  Department of Mechanical Engineering, University of Minho, Campus of Azurém, 4800-058 Guimarães, Portugal; E-Mails: a53996@alumni.uminho.pt (V.C.); a61938@alumni.uminho.pt (V.V.)

†  These authors contributed equally to this work.

\*  Author to whom correspondence should be addressed; E-Mail: puga@dem.uminho.pt; Tel.: +351-253-510-220; Fax: +351-253-516-007.

Academic Editor: Hugo F. Lopez

**Abstract:** The present study evaluates the effect of high-intensity ultrasound (US) in the static and dynamic mechanical behavior of AZ91D by microstructural modification. The characterization of samples revealed that US treatment promoted the refinement of dendrite cell size, reduced the thickness, and changed the $\beta$-$Mg_{17}Al_{12}$ intermetallic phase to a globular shape, promoted its uniform distribution along the grain boundaries and reduced the level of porosity. In addition to microstructure refinement, US treatment improved the alloy mechanical properties, namely the ultimate tensile strength (40.7%) and extension (150%) by comparison with values obtained for castings produced without US vibration. Moreover, it is suggested that the internal friction, enhanced by the reduction of grain size, is compensated by the homogenization of the secondary phase and reduction of porosity. It seems that by the use of US treatment, it is possible to enhance static mechanical properties without compromising the damping properties in AZ91D alloys.

## 1. Introduction

Mg alloys are a promising candidate for applications involving low-weight and high-damping characteristics. Metallic materials have relatively low damping, although Mg alloys, in addition to their very low density, possess the highest damping capacity among metals [1]. However, they are characterized by a relatively low elastic modulus and mechanical strength. This dependence between static and dynamic mechanical properties is a common feature of metals, given that high-damping materials are generally unsuitable in many structural applications [2]. Since, the referred mechanical properties are dependent on the material's microstructure and bulk defects, Mg alloy processing is the main route to manipulate both static and dynamic properties. Enhanced static mechanical properties, *i.e.*, elevated values of yield/ultimate strength and fracture extension, are generally correlated with the microstructure of a given material and the presence of bulk defects. For instance, the values of plastic flow stress ($\sigma_y$) is related to the grain size (*d*) by the Hall-Petch relation [3]:

$$\sigma_y = \sigma_0 + k_y d^{-1/2} \tag{1}$$

where $\sigma_0$ is the friction stress of mobile dislocations and $k_y$ defines the characteristic constant that depends on the amount of impurities and alloying elements [3]. Additionally, the values of ultimate tensile strength and fracture extension can be diminished by the presence of porosities, which are promoters of stress concentration and crack nucleation in bulk materials [4].

As for the dynamic mechanical properties, it is desirable to obtain materials with high damping properties, *i.e.*, a high ability to dissipate elastic strain energy during mechanical vibration or wave propagation [2]. This energy dissipation is promoted by the internal friction generated through inelastic relaxation and/or thermal activation. The presence of point defect relaxation, dislocation mechanisms, interfaces, and their combination with thermal activation processes are the main cause of internal friction. Consequently, they are associated with the morphology of the microstructure, namely by the secondary phases, impurity atoms [5], porosity, grain size, and boundaries [5,6]. This internal friction has a relevant role in the viscoelastic behavior of materials and consequently implies a lag time effect that is generally neglected by the classical Hooke's law formulation. According to Equation (2), the overall strain ($\varepsilon$) is composed by two terms, an elastic strain ($\varepsilon_e$) and an inelastic strain ($\varepsilon_a$) [7]:

$$\varepsilon = \varepsilon_e + \varepsilon_a \tag{2}$$

The instant stress ($\sigma$) and strain values under cyclic loading can be described by Equations (3) and (4) [7]:

$$\sigma = \sigma_0{}^{i\omega t} \tag{3}$$

$$\varepsilon = \varepsilon_0{}^{i(\omega t - \phi)} \tag{4}$$

where $\sigma_0$ and $\varepsilon_0$ are, respectively, the original stress and strain amplitudes, $\omega$ is the circular frequency, *t* the time, and $\phi$ is the loss angle by which the strain lag is delayed relatively to the stress. These two factors are correlated to the material complex modulus ($E^*$), that can be defined by a dissipated energy part (loss modulus, $E''$) and a stored energy part (storage modulus, $E'$) according to Equation (5). The ratio between the dissipated and stored energies is the internal friction ($Q^{-1}$) of the material, which can be determined by the use of Equation (6) [8]:

$$E* = \frac{\sigma}{\varepsilon} = E' + iE'' \tag{5}$$

$$Q^{-1} = \frac{E''}{E'} \tag{6}$$

The value of internal friction is known to be associated with the dislocation properties of metals [9] at low temperatures and with thermal energy at high temperatures, according to thermodynamics and Granato-Lücke dislocation theory [10]. According to Hu *et al.* [11], at room temperature, Mg alloys' internal friction is related to dislocations, while at elevated temperatures some crystal defects must be thermally activated to enhance damping.

From the classical work of Granato and Lücke [12], internal friction due to dislocation mechanism is strain dependent, and the logarithmic decrement δ is characterized by two parts, according to Equation (7) [13]:

$$\delta = \delta_0 + \delta_H(\varepsilon) \tag{7}$$

For low values of strain, the value of internal friction is strain-independent and assumes the value of $\delta_0$. If the strain amplitude values are increase, higher than the material critical strain ($\varepsilon_{cr}$), the internal friction becomes strain-dependent and increases exponentially. The strain-independent internal friction is the result of reversible movements of dislocation and microscopic yielding [14] around the initial pinned positions and is associated to the values obtained by the application of Equation (8) [13]:

$$\delta_0 \sim \rho l^4 \tag{8}$$

where ρ is the dislocation density and *l* is the mean length of dislocation between the weak pinning points [15]. Dislocation damping can be enhanced by thermal activation. Thermal currents and the stress generated by inhomogenities and individual anisotropic elastic crystals enhance damping in macroscopic polycrystalline metals [16]. This activation, promoted by external thermal energy, is dependent to the temperature, frequency, impurities, and microstructural morphology [17]. It may be observed that the main intrinsic factor related to the static and dynamic mechanical behavior is related with to the microstructure, namely the grain size and boundaries, presence of impurities, secondary phases, and porosity. Thus, in order to optimize material characteristics, it is essential to processes materials to manipulate their microstructure.

The microstructural refinement of Mg alloys can be performed by two basic approaches: (i) thermomechanical treatment through plastic deformation in which dynamic recrystallization leads to the formation of small equiaxed grains [18]; (ii) casting processing where two different routes can be followed: chemical [19] or physical [20–22] treatment. An example of physical processing is the application of ultrasound treatment [23]. Although the effect of refinement by ultrasound in molten metal has been studied [24], this subject has been mainly explored on the effects of ultrasonic vibration in the microstructure and only few works have focused the effect in the dynamic mechanical properties.

This paper presents and discusses the effect of ultrasonic treatment in the microstructure and the static/dynamic mechanical behavior of AZ91D alloy cast in a permanent mold by applying ultrasound indirectly to the melt during the first stages of solidification.

## 2. Experimental Section

The experimental set-up used to perform ultrasonic refinement consisted on a MMM (Multi-frequency Multimode Modulated—MPI, Le Locle, Switzerland) technology US power supply unit, a high power ultrasonic generator (3000 W), a $\varnothing$ 38.1 mm $\times$ 92 mm $Ti_6Al_4V$ long acoustic waveguide, an acoustic load composed by a steel die ($\varnothing$ 24 mm $\times$ 120 mm long) and the liquid metal, according to Figure 1a. The MMM technology is characterized by synchronously exciting many vibration modes through the coupled harmonics and sub-harmonics in solids and liquid containers, to produce high intensity multimode vibration that are uniform and repeatable, which avoid the creation of stationary and standing waves, so that the whole vibrating system is fully agitated, improving the degassing and refinement process. The equipment is fully controlled through Windows compatible software developed by MPI (Le Locle, Switzerland).
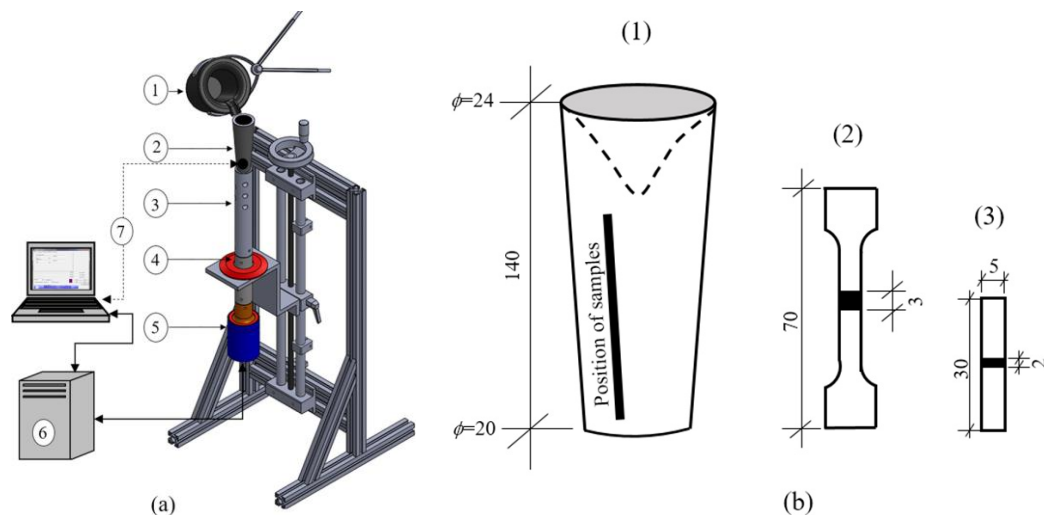
**Figure 1.** (**a**) Experimental setup: (1) crucible, (2) steel die, (3) waveguide, (4) booster and (5) 20 kHz Ttransducer, (6) MMM generator, (7) thermocouple sensor; (**b**) casted specimens: (1) casting, (2) tensile sample and (3) DMA sample.

The AZ91D alloy (whose chemical composition is presented in Table 1) was melted and held inside the crucible at 700 °C for 15 min for homogenization while protected by $CO_2 + 0.5\%$ $SF_6$ atmosphere to prevent the oxidation. The molten alloy was then allowed to cool to 680 °C and poured in the steel die (pre-heated to 250 °C). For every experimental condition, US vibration regulated for 400 W and $20.1 \pm 0.25$ kHz frequency was continuously applied to the bottom of the die until solidus $\pm 10$ °C and then stopped, allowing the melt to cool to room temperature. For the sake of comparison the alloy was also poured without ultrasonic vibration.

Specimens for microstructure characterization were taken from cast samples (Figure 1b(1)), by sectioning them perpendicularly to its longitudinal axis, at a distance of 60 mm to the waveguide/mold interface. The samples were etched in a solution containing 1 mL glacial acetic acid, 50 mL distilled water, and 150 mL anhydrous ethyl alcohol. The porosity was determined by the use of an image editing software (ImageJ) where a contrast tool was applied to reveal the fraction of area covered by pores in five image fields by processing conditions, with a magnification of $100\times$.

**Table 1.** Composition of the AZ91D Mg alloy used in this work, obtained by optical emission spectrometry.

| Element | wt. % |
|---------|-------|
| Al | 9.100 |
| Zn | 0.850 |
| Mn | 0.150 |
| Fe | 0.005 |
| Cu | 0.003 |
| Ni | 0.002 |
| Si | 0.050 |
| Other | 0.030 |
| Mg | Bal. |

To characterize the static mechanical behavior for both experimental conditions, specimens (10 of each processing conditions) were machined from the as-cast samples with a gauge length $L_0$ of 40 mm and a rectangular cross section of $5 \times 3$ mm$^2$ (Figure 1b(2)). Tensile tests were carried out at room temperature with 0.02 s$^{-1}$ strain rate. Vickers hardness measurements were performed on the as-cast US treated and non-treated samples. Ten measurements were performed for each processing, using a 5 kgf load and 20 s dwell.

To determine the dynamic thermomechanical behavior, the $30 \times 5 \times 2$ mm$^3$ rectangular samples (Figure 1b(3)) were tested using Dynamic Mechanical Analysis in a single-cantilever configuration. This type of test applies a sinusoidal load to the sample and monitors the resultant deformation, evaluating the energy accumulated in the material ($E'$, storage modulus) and the energy that is lost in that process ($E''$, loss modulus). Consequently, the damping capacity of the material can be evaluated determining its internal friction ($Q^{-1}$), according to Equation 6 [25]. The samples were tested using a $4 \times 10^{-4}$ mm/mm strain amplitude, at 0.5, 10, and 20 Hz frequencies while heated at 10 ℃/min from room temperature to 300 ℃ in nitrogen atmosphere. The strain amplitude value was selected to obtain damping values related to the strain independent region above the value of critical strain [26] and the adopted frequency values have been shown to reveal the viscous manner in grain boundaries at elevated temperatures [14].

## 3. Results and Discussion

Figure 2 shows the microstructure of as-cast AZ91D alloy for both non-treated and US treated specimens. The specimens treated by US (Figure 2b,d) reveal a more refined grain structure and homogeneous α-Mg matrix, when compared with the non-treated (Figure 2a,c) specimens. According to these microstructures, the supply of acoustic energy to the melt during the solidification has a high potential to change the morphology of the β-Mg$_{17}$Al$_{12}$ intermetallic phase (the predominant intermetallic phase present in the alloy grain boundaries [26]).

US treatment promotes a uniform dispersion in the matrix along the grain boundaries, as already demonstrated in previous works [27]. The efficiency of this refinement, caused by the effect of US, can be attributed to cavitation by two distinct mechanisms: (i) heterogeneous nucleation at high (above liquidus) temperature, and (ii) intermetallic compound fragmentation due to the streaming acoustic effect. The co-existence of two mechanisms, during the stage of solidification under effect of ultrasonic

vibration, suggests an enhanced refinement of dendrite cell size, thinning, and dispersion of β-Mg$_{17}$Al$_{12}$ intermetallic phase in the α-Mg matrix. The β-Mg$_{17}$Al$_{12}$ intermetallic is confirmed by the SEM/EDS analysis presented in Figures 3 and 4.
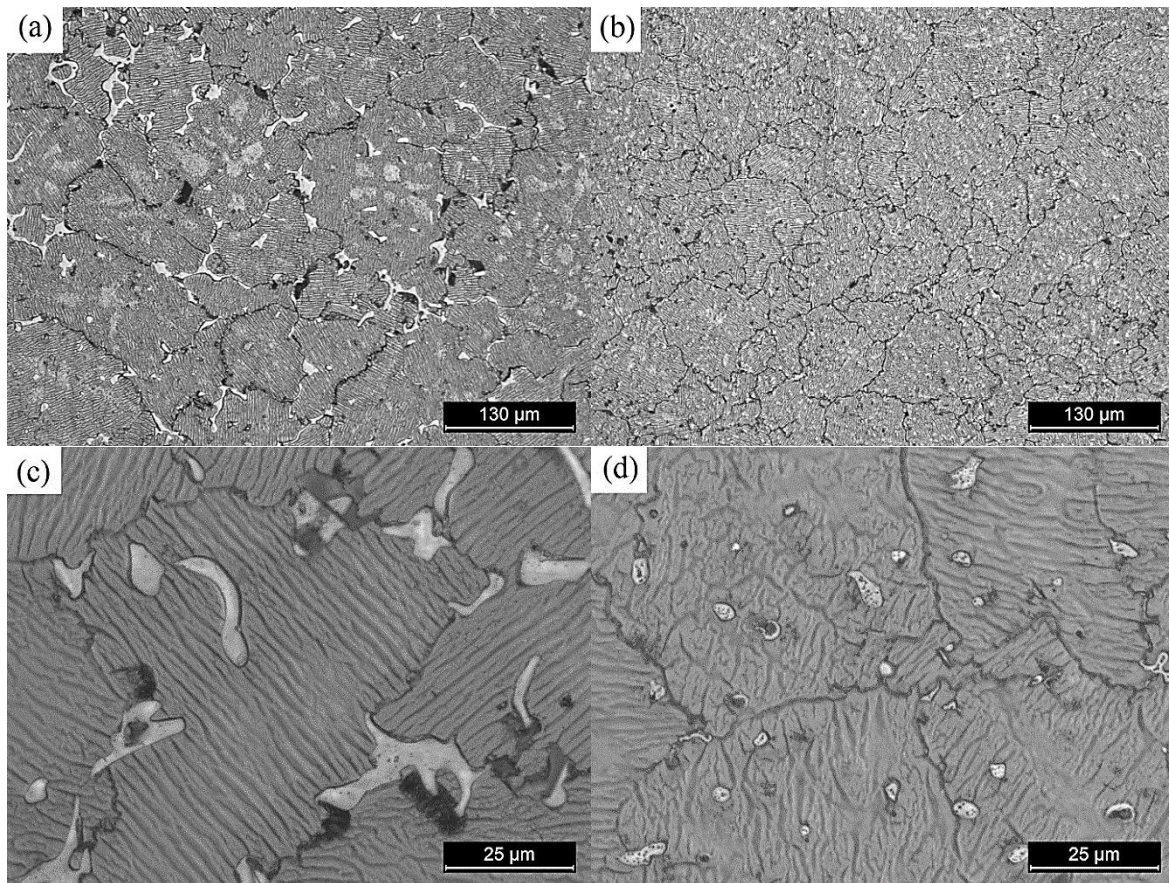


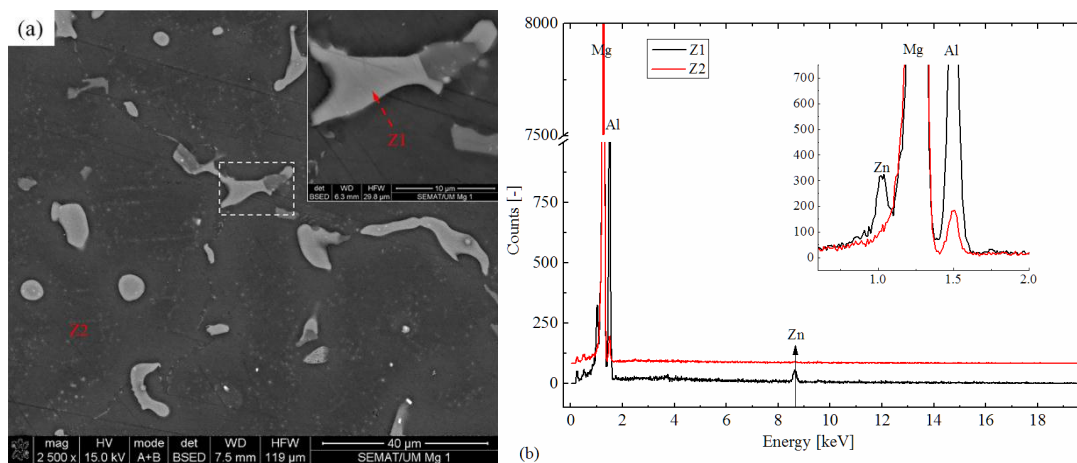**Figure 2.** As-cast microstructures of AZ91D: (**a**,**c**) non-treated samples; (**b**,**d**) US treated samples.



**Figure 3.** (**a**) Morphology and distribution of the β-Mg$_{17}$Al$_{12}$ intermetallic phase in non-treated samples; and (**b**) EDS spectrum of the β-Mg$_{17}$Al$_{12}$ intermetallic phase.
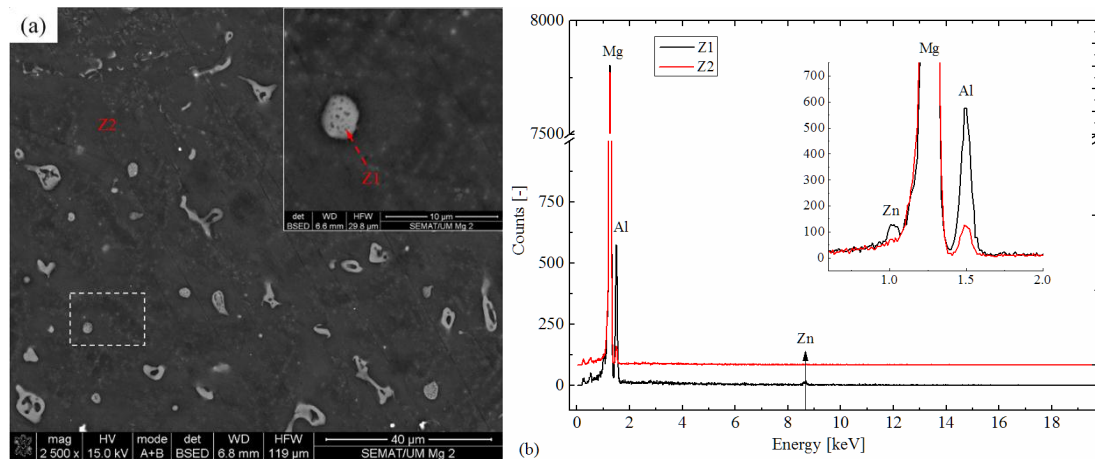
**Figure 4.** (**a**) Morphology and distribution of the β-Mg$_{17}$Al$_{12}$ intermetallic phase in US treated samples; and (**b**) EDS spectrum of the β-Mg$_{17}$Al$_{12}$ intermetallic phase.

Additionally to the microstructure refinement, US treatment also has a great impact on the porosity of Mg alloys [28]. Observing the microstructure shown in Figure 2a and according to Table 2, it is evident that the level of porosity is lower in US treated samples. The reduction of porosity in samples processed by US can be attributed to the effect of acoustic cavitation developed in the molten metal during the first stage of solidification.

**Table 2.** Characteristics of the microstructures.

| Samples | Grain Size ∅ (µm) | Porosity (Area %) | β-Mg$_{17}$Al$_{12}$ | |
| --- | --- | --- | --- | --- |
| | | | Area % | Morphology |
| Non-treated | 120 ±20 | 2.1 ±0.3 | 5.45 ±0.5 | Coarse with blocky shape |
| US treated | 64 ±5 | 0.8 ±0.1 | 5.67 ±0.4 | Fine with globular shape |

Figure 5 represents the mean static mechanical properties of the as-cast AZ91D alloy for both non-treated and US treated specimens, by showing their stress-strain curve. From this figure it is evident that US treatment effectively enhanced the ultimate tensile strength and the elongation of the material. Non-treated samples are characterized by an average tensile strength of 160 MPa, being increased to 225 MPa after US treatment. Additionally, an increase in elongation was also verified, which allowed an enhancement in toughness of approximately four times when compared with non-treated samples.

It is well known that static mechanical properties of Mg alloys depend on several factors, with particular emphasis to the microstructure morphology [29], presence of intermetallic phases [30], and porosity [28,29]. Focusing on the β-Mg$_{17}$Al$_{12}$ intermetallic phase, Li *et al*. [10] pointed that the body-centered cubic structure can deteriorate the ultimate tensile strength and elongation. Moreover, according to Du *et al*. [29] the uniform distribution of fine β-Mg$_{17}$Al$_{12}$ intermetallic phase enhances mechanical properties. The same authors also refer that the main defects that lower mechanical properties are gas pores and microstructural non-uniformity. The reduction of these defects contributes for the reduction of the stress concentration in the bulk material, thus improving ductility by the prevention of early fracture. This enhancement in ductility promoted by US treatment can be confirmed by the superior hardness values of the treated samples (78 ±4 HV$_5$) when compared with non-treated samples (65 ±6 HV$_5$).
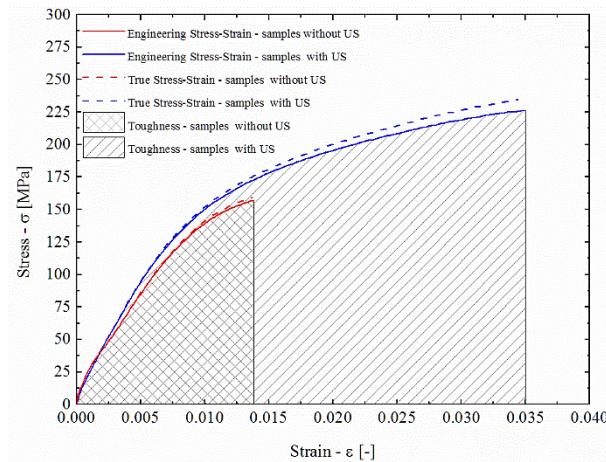
**Figure 5.** Mean static mechanical properties of as-cast AZ91 D alloy for both non-treated and US treated specimens.

According to Figure 2d and Table 2, it is suggested that the US treatment reduced the size of $\beta$-$Mg_{17}Al_{12}$ phase, promoted a globular shape and improved their uniformity and distribution in the $\alpha$-Mg matrix. It seems that the mechanism through which the US treatment affects the size and shape of the intermetallic phase depends on the solidification process under ultrasonic vibration. As the US treatment was performed continuously from the pouring temperature until solidus ($\pm 10$ ℃), the results can be explained as a conjugation of two mechanisms: cavitation-enhanced heterogeneous nucleation (of both grain and intermetallic phase) and the fragmentation of the $\beta$-$Mg_{17}Al_{12}$ phase.

During the first stage of solidification, the US treatment improves the grain refinement by heterogeneous nucleation, as well as the wettability of the $\beta$-$Mg_{17}Al_{12}$ by the metal further improving the refinement of the secondary phase. On a second stage, corresponding to the formation of the first solid metal, the cavitation can develop acoustic streaming caused by the collapse of the bubbles in the remaining liquid, promoting the fragmentation of grain dendrites and intermetallic clusters.

The coexistence of these two mechanisms seems to promote a high density of nuclei in the melt, thus, leading to the development of a large number of smaller grains [23]. These aspects are in agreement with this work, in which uniformity of microstructure, reduced porosity and refinement of $\beta$-$Mg_{17}Al_{12}$ intermetallic phase promoted the increase of static mechanical properties.

The internal friction of AZ91D is presented in Figure 6. It is shown that the frequency effect is not relevant at room temperature, however with increasing temperature the value internal friction tends to increase at a higher rate for low frequencies, as confirmed by the increase in the curves slope.

Observing the damping behavior shown in Figure 6, it can be seen that temperature increase generates an elevation in the internal friction in the samples, however, this effect is more pronounced for lower frequencies (0.5 Hz). At higher frequencies (10 and 20 Hz) it is suggested that there is no significant difference in terms of internal friction. This behavior was already confirmed previously in AZ91 alloys by Shu-wei Liu *et al*. [31]. Interpreting Figure 6, there seems to be no significant difference in terms of internal friction between US treated and non-treated samples.

It is known that the major source of internal friction in Mg alloys is the dislocation motion of basal planes in the hexagonal structure by stress induced inelasticity [32] and this movements are dependent to the grains size [33] and shape [34], presence of secondary phases [35], and porosity [10].
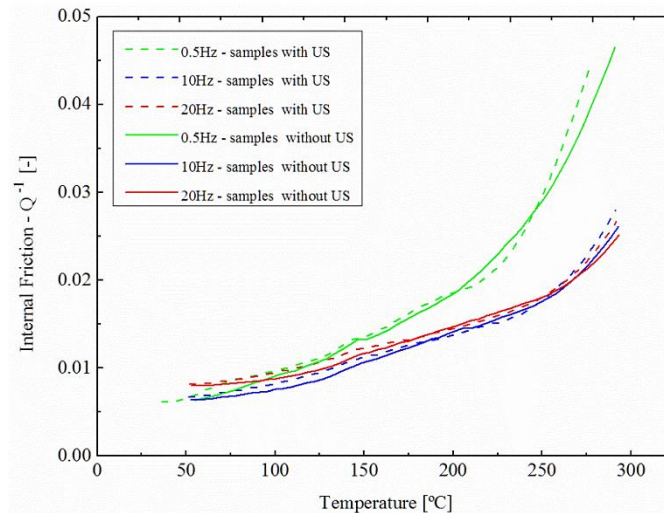
**Figure 6.** Internal friction ($Q^{-1}$) of as-cast AZ91D.

According to Figure 2b and Table 2, it can be observed that the grain size is reduced by US treatment and this is generally a route to enhance internal friction [13]. However, US treatment promotes the dispersion and homogenization of the secondary phase β-$Mg_{17}Al_{12}$ and a reduction of porosity in the bulk samples, and those are primary sources in internal friction by dislocation motion. The dispersion of β-$Mg_{17}Al_{12}$ and reduction of porosity implies the reduction of viscous flow and a loss in the dissipated energy under cyclic stress. Additionally, the homogenization of the grain shape by US treatment involves the reduction of dendrite grains, another source of internal friction due to high angular in the vicinity of boundaries. Since one of the fundamental damping mechanisms in polycrystals is originated by dislocation on grain boundaries and between the primary (α-Mg) and secondary (β-$Mg_{17}Al_{12}$) phases, rather than lattice dislocations in the grain interior [6], there are opposite damping transformations generated by US treatment.

Figure 7a presents the damping peaks extracted from the plots in Figure 6, originated by activation of thermoelastic effects [10]. Considering the values of peak damping, it may be observed that US treatment enhances the internal friction at lower frequencies. Additionally, it can be observed that with an increase in frequency promotes a narrowing of the damping peak in US treated samples, relative to the non-treated samples. It is visible that an increase in frequency generates an elevation in the peak temperature, however, it seems that US treatment has no relevant role in the change of peak temperature.

Figure 7b shows the Arrhenius plot of both US treated and non-treated samples. It can be observed by the slopes of the functions, that US treated samples shows an activation energy of 1.73 eV, while non-treated as-cast samples reveal an activation energy of 1.82 eV. Apparently, US-treatment has no relevant effect on the activation energy in AZ91D alloys.

According to the results, it is suggested that the enhancement of internal friction by the reduction of grain size is compensated by the dispersion of the intermetallic phase, grain homogenization and reduction of porosity generated by the US treatment. Thus, even though US treatment promotes a significant change in the material microstructure there is no relevant changes in the bulk dynamic mechanical properties of the AZ91D alloy.
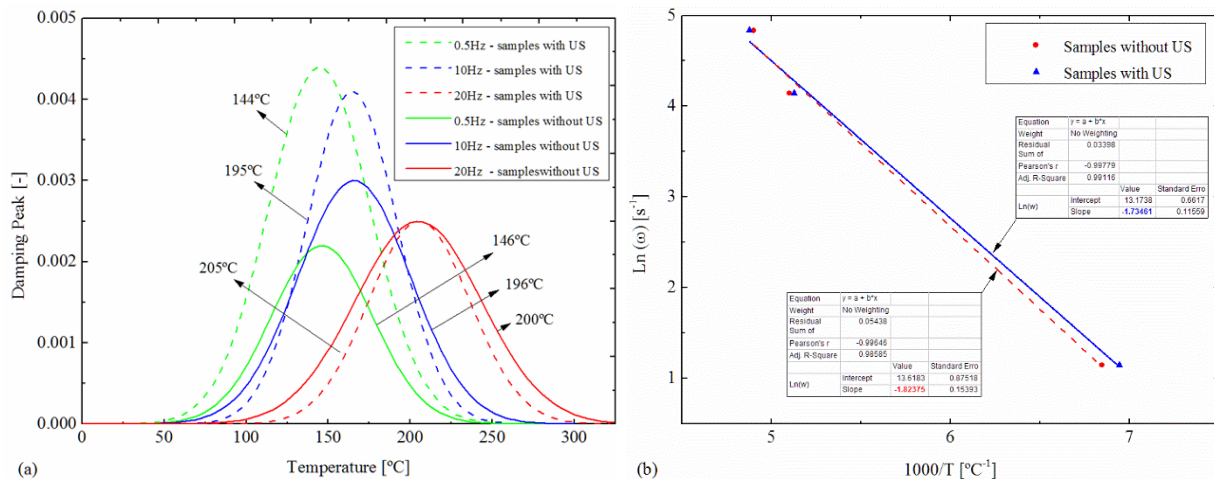
**Figure 7.** Damping peaks (**a**) and Arrhenius plot (**b**) in AZ91 alloy.

## 4. Conclusions

(1). The effect of US treatment during solidification refines the α-Mg matrix and β-Mg₁₇Al₁₂ intermetallic phase.

(2). The use of high intensity acoustic vibration promotes uniform dispersion of the β-Mg₁₇Al₁₂ intermetallic phase and reduces the level of porosity.

(3). Static tensile testing shows an increase of both tensile strength (40.7%) and strain (150%) when processing the alloys by US. Consequently, the overall toughness in US processed as-cast samples is increased by four times.

(4). US treated samples show an activation energy of 1.73 eV, while non-treated samples reveal an activation energy of 1.82 eV. It suggested that the internal friction, generated by the grain refinement by US treatment, is compensated by a loss of damping capacity due to the intermetallic phase dispersion and reduction porosity.

(5). US treatment in the AZ91D samples seems to improve static mechanical properties without compromising the dynamic mechanical properties of these alloys.

## Acknowledgments

## Author Contributions

H.P. and V.C. conceived and designed the experiments, wrote and edited the manuscript, and contributed in all activities. V.V. performed OM and SEM experiment. J.B. helped finishing casting experiments, analyzing the results and revising the manuscript.

## Conflicts of Interest

The authors declare no conflict of interest.

## References

1. James, D.W. High damping metals for engineering applications. *Mater. Sci. Eng.* **1969**, *4*, 1–8.
2. Zhang, J.; Perez, R.J.; Lavernia, E.J. Documentation of damping capacity of metallic, ceramic and metal-matrix composite materials. *J. Mater. Sci.* **1993**, *28*, 2395–2404.
3. Ono, N.; Nowak, R.; Miura, S. Effect of deformation temperature on Hall-Petch relationship registered for polycrystalline magnesium. *Mater. Lett.* **2004**, *58*, 39–43.
4. Li, X.; Xiong, S.M.; Guo, Z. Correlation between Porosity and Fracture Mechanism in High Pressure Die Casting of AM60B Alloy. *J. Mater. Sci. Technol.*, in press, 2015.
5. Colakoglu, M. Factors effecting internal damping in aluminium. *J. Theor. Appl. Mech.* **2004**, *42*, 95–105.
6. Jiang, W.B.; Kong, Q.P.; Cui, P. Further evidence of grain boundary internal friction in bicrystals. *Mater. Sci. Eng. A* **2010**, *527*, 6028–6032.
7. Blanter, M.S; Golovin, I.S.; Neuhauser, H.; Sinning, H.-R. *Internal Friction in Metallic Materials: A Handbook*; Springer: Berlin, Germany, 2007.
8. Liu, C.; Pineda, E.; Crespo, D. Mechanical Relaxation of Metallic Glasses: An Overview of Experimental Data and Theoretical Models. *Metals* **2015**, *5*, 1073–1111.
9. Filmer, A.J.; Hutton, G.J.; Hutchison, T.S. Internal Friction in Aluminum at Low Temperatures. *J. Appl. Phys.* **1958**, doi:10.1063/1.1723055.
10. Zhang, J.; Gungor, M.N.; Lavernia, E.J. The effect of porosity on the microstructural damping response of 6061 aluminium alloy. *J. Mater. Sci.* **1993**, *28*, 1515–1524.
11. Hu, X.; Wang, X.; He, X.; Wu, K.; Zheng, M. Low frequency damping capacities of commercial pure magnesium. *Trans. Nonferrous Met. Soc. China* **2012**, *22*, 1907–1911.
12. Granato, A.; Lücke, K. Theory of Mechanical Damping Due to Dislocations. *J. Appl. Phys.* **1956**, doi:10.1063/1.1722436.
13. Liao, L.; Zhang, X.; Li, X.; Wang, H.; Ma, N. Effect of silicon on damping capacities of pure magnesium and magnesium alloys. *Mater. Lett.* **2007**, *61*, 231–234.
14. Watanabe, H.; Owashi, A.; Uesugi, T.; Takigawa, Y.; Higashi, K. Grain boundary relaxation in fine-grained magnesium solid solutions. *Philos. Mag.* **2011**, *91*, 4158–4171.
15. Fan, G.D.; Zheng, M.Y.; Hu, X.S.; Wu, K.; Gan, W.M.; Brokmeier, H.G. Internal friction and microplastic deformation behavior of pure magnesium processed by equal channel angular pressing. *Mater. Sci. Eng. A* **2013**, *561*, 100–108.
16. Randall, R.H.; Zener, C. Internal Friction of Aluminum. *Phys. Rev.* **1940**, *58*, 472–473.
17. Cao, X.; Huang, C. The annealing and aging effects of high temperature internal friction in pure aluminum. *Mater. Sci. Eng. A* **2004**, *383*, 341–346.
18. Chen, Y.; Wang, Q.; Lin, J.; Liu, M.; Hjelen, J.; Roven, H.J. Grain refinement of magnesium alloys processed by severe plastic deformation. *Trans. Nonferrous Met. Soc. China* **2014**, *24*, 3747–3754.

19. Lee, Y.C.; Dahle, A.K.; StJohn, D.H. The role of solute in grain refinement of magnesium. *Metall. Mater. Trans. A* **2000**, *31*, 2895–2906.

20. Liu, X.; Osawa, Y.; Takamori, S.; Mukai, T. Grain refinement of AZ91 alloy by introducing ultrasonic vibration during solidification. *Mater. Lett.* **2008**, *62*, 2872–2875.

21. Eskin, G.I.; Eskin, D.G. *Ultrasonic Treatment of Light Alloy Melts*, 2nd ed.; CRC Press: Boca Raton, FL, USA, 2014.

22. Ali, Y.; Qiu, D.; Jiang, B.; Pan, F.; Zhang, M.-X. Current research progress in grain refinement of cast magnesium alloys: A review article. *J. Alloys Compd.* **2015**, *619*, 639–651.

23. Puga, H.; Barbosa, J.; Costa, S.; Ribeiro, S.; Pinto, A.M.P.; Prokic, M. Influence of indirect ultrasonic vibration on the microstructure and mechanical behavior of Al–Si–Cu alloy. *Mater. Sci. Eng. A* **2013**, *560*, 589–595.

24. Ferguson, J.; Schultz, B.; Cho, K.; Rohatgi, P. Correlation *vs.* Causation: The Effects of Ultrasonic Melt Treatment on Cast Metal Grain Size. *Metals* **2014**, *4*, 477–489.

25. Anilchandra, A.R.; Surappa, M.K. Microstructure and damping behaviour of consolidated magnesium chips. *Mater. Sci. Eng. A* **2012**, *542*, 94–103.

26. Zhang, Z.; Zeng, X.; Ding, W. The influence of heat treatment on damping response of AZ91D magnesium alloy. *Mater. Sci. Eng. A* **2005**, *392*, 150–155.

27. Patel, B.; Chaudhari, G.P.; Bhingole, P.P. Microstructural evolution in ultrasonicated AS41 magnesium alloy. *Mater. Lett.* **2012**, *66*, 335–338.

28. Liu, X.; Zhang, Z.; Hu, W.; Le, Q.; Bao, L.; Cui, J.; Jiang, J. Study on hydrogen removal of AZ91 alloys using ultrasonic argon degassing process. *Ultrason. Sonochem.* **2015**, *26*, 73–80.

29. Du, X.; Zhang, E. Microstructure and mechanical behaviour of semi-solid die-casting AZ91D magnesium alloy. *Mater. Lett.* **2007**, *61*, 2333–2337.

30. Li, P.; Tang, B.; Kandalova, E.G. Microstructure and properties of AZ91D alloy with Ca additions. *Mater. Lett.* **2005**, *59*, 671–675.

31. Liu, S.; Jiang, H.; Li, X.; Rong, L. Effect of precipitation on internal friction of AZ91 magnesium alloy. *Trans. Nonferrous Met. Soc. China.* **2010**, *20*, s453–s457.

32. Schwaneke, A.; Nash, R. Effect of preferred orientation on the damping capacity of magnesium alloys. *Metall. Mater. Trans. B* **1971**, *2*, 3453–3457.

33. Wang, H.; Tian, X.-F.; Yin, C.; Huang, Z. The effect of heat treatment and grain size on magnetomechanical damping properties of Fe–13Cr–2Al–1Si alloy. *Mater. Sci. Eng. A* **2014**, *619*, 199–204.

34. Nowick, A.S. Dislocations and Crystal Boundaries. In *Anelastic Relaxation in Crystalline Solids*; Academic Press: New York, NY, USA, 1972; pp. 350–370.

35. Tanaka, M.; Iizuka, H. Effects of grain size and microstructures on the internal friction and Young's modulus of a high-strength steel HT-80. *J. Mater. Sci.* **1991**, *26*, 4389–4393.